

Rocket propulsion, materials & integrated circuits



Index

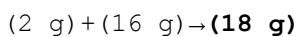
- Mechanisms
- Variables
- Materials(simulation-metals, steel)
- Integration of circuit design in VHDL
- Algorithms

(In this text I will describe the structure of the variables to compute in a specific program modeling (Pyrocket) in order to be concise and clear in the variables of fuel, mass, carbon, hydrocarbures, air, pressure...)

Mechanisms

In a rocket engine, propellant is burnt to produce high-temperature and high-pressure gas while undergoing chemical reactions. In the chemical reaction, mass balance describing exactly how much oxidizer has to be supplied for complete combustion of a certain amount of fuel is generally termed as stoichiometry.

Measures;



1 mol of hydrogen is reacted with **1/2 mol of oxygen** to produce 1 mol of water. Note that this is a balanced equation in which numbers of chemical elements are balanced. It is interesting to note that **2 g of hydrogen can react with 16 g of oxygen to produce 18 g** of water. That means the mass in the left side of reaction is the same as that in the right side, thus stating that mass is conserved.

Measures;

$$\frac{(A/B)}{76} = \frac{(\text{fuel})}{([m]_{\text{air}}/[R]_{\text{fuel}})} = 4$$

el are the molecular weights of air and fuel, respectively. The stoichiometric air-fuel ratio can be obtained using the variables [m] & [R] for any hydrocarbon fuels such as for methane, propane, butane.

Aerothermochemistry of Rocket Engines:

The actual measured properties of solid and liquid substances can be used, which can be expressed in the form of the thermodynamic equation of state.

The variables are P, the pressure V is the volume of the gas T is the temperature of the gas n is the number of moles of gas Ru is the universal gas constant (**Ru = 8.314 kJ/kmol K**)

Compute these variables with python:

```
PV n = R T
Mol => m m tot A = +m m
Mass => = + Y Y A B + + Y Y C i + = ΣY
```

We are calculating variables, the mass, the pressure constant and the combustible-air relations To compute all of the magnitudes with Python.

Mass-fractions

YA(= mA/mtot) is the mass fraction of species A. It can be noted that the sum of all mass fraction of individual species in a mixture is equal to unity:

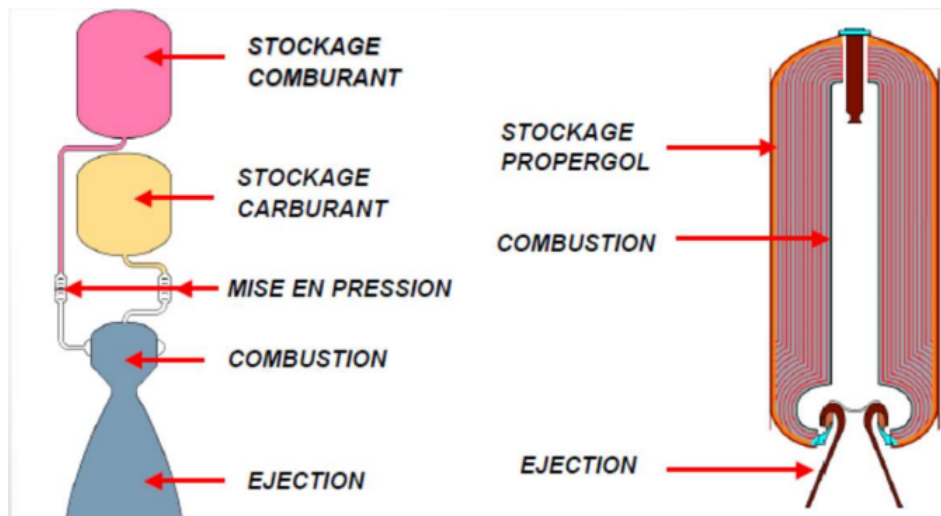
“By total number of moles, ntot variable, we will get these variables to compute”

$$n_{\text{tot}} = \sum_i n_i$$

$$1 = \sum_i \frac{X_i}{M_i} = \sum_i \frac{Y_i}{M_i}$$

The mole fraction X_i and mass fraction Y_i : MW_i is the molecular weight of i th species. The mixture molecular weight can be easily estimated by knowing either species mole or mass fractions.

$$Y_{mn} = \frac{M_n}{\sum_i M_i X_i} = \frac{M_n}{M_{\text{mix}}}$$



MW_i is the molecular weight of a species. The mixture molecular weight can be easily estimated by knowing either species mole or mass fractions and by other hand, the constant pressure (P) of gaseous mixture is the sum of the pressure that each component would exert if it alone occupies the same volume of mixture at the same temperature of the mixture.

$$p_i = X_i P$$

The specific internal energy u of the mixture can be determined from a knowledge of their respective values of the constituent species. The variables are $[u_i]$ is the internal energy of i th species per unit mole $[u_i]$ is the internal energy of i th species per unit mass.

The **enthalpy** variables to compute:

$$h_{i,T}^0(T) = h_{f,298.15}^0 + \int_{298.15}^T C_{P,i} dT$$

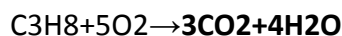
Fundamentals of Rocket Propulsion:

Note that the enthalpy of any species at particular temperature is composed of two parts: (1) the heat of formation, which represents the sum of enthalpy due to chemical energy associated with chemical bonds; and (2) sensible enthalpy, as it is associated with temperature.

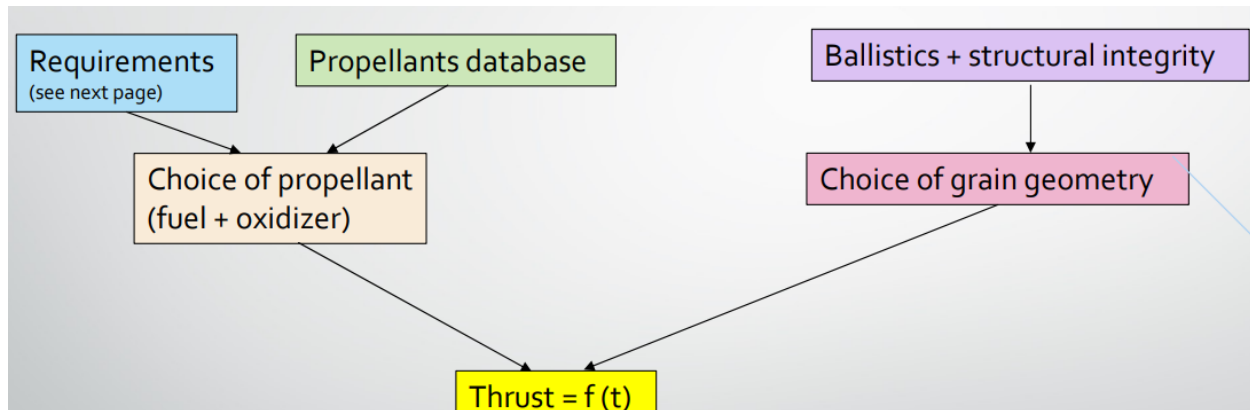
In the combustion process, several chemical reactions take place simultaneously. In some reactions, heat will be evolved and in others, heat will be absorbed. The heat formation of a particular species can be defined as the heat of reaction per mole of product formed isothermally from elements in their standard states.

Chemical Formula	Species Name	State	Standard Heat of Formation (kJ/mol)
O ₂	Oxygen	Gas	0.0
O	Element oxygen	Gas	247.4
H ₂	Hydrogen	Gas	0.0
H	Element hydrogen	Gas	218.1
OH	Hydroxyl	Gas	42.3
H ₂ O	Water	Gas	-242.0
H ₂ O	Water	Liquid	-286.0
C	Graphite	Solid	0.0
CO	Carbon monoxide	Gas	-110.5
CO ₂	Carbon dioxide	Gas	-394.0
CH ₄	Methane	Gas	-74.5
C ₃ H ₈	Propane	Gas	-103.8
C ₄ H ₁₀	Butane(n)	Gas	-124.7
C ₄ H ₁₀	Butane(iso)	Gas	-131.8
C ₂ H ₂	Acetylene	Gas	226.9
N ₂	Nitrogen	Gas	0
H ₂ O	Water	Gas	-242.0
H ₂ O	Water	Liquid	-272.0

The heat of reaction can be defined as the difference between the enthalpy of the products and enthalpy of reactants at the specified states. liberating a certain amount of heat, then the heat of reaction is known as the heat of combustion.



Estimate the higher and lower heating values at 298 K of LPG (Propane = 70%, Butane = 30%) per mole and per kilogram of fuel.



Estimation-variables

$$\bar{h}_{f,\text{CO}_2}^0(g) = -393.522 \text{ kJ/mol}$$

$$\bar{h}_{f,\text{H}_2\text{O}}^0(l) = -286.000 \text{ kJ/mol for (HHV)}$$

$$\bar{h}_{f,\text{H}_2\text{O}}^0(g) = -241.826 \text{ kJ/mol for LHV}$$

$$\bar{h}_{f,\text{C}_3\text{H}_8}^0 = -103.92 \text{ kJ/mol}$$

$$\bar{h}_{f,\text{C}_4\text{H}_{10}}^0 = -124.733 \text{ kJ/mol}$$

HHV = -393.522 kJ/mol for CO₂(g), -286.000 kJ/mol for H₂O(l), -241.826 kJ/mol for H₂O(g), -103.92 kJ/mol for C₃H₈(g), -124.733 kJ/mol for C₄H₁₀(g). HHV kJ/mol

The theoretical/ideal flame temperature during combustion process for a particular fuel–air ratio, provided no heat liberated can be transferred from its system boundary. (The equilibrium state) by constant pressure and adiabatic process. The final temperature attained by the system is known as adiabatic flame temperature T_{ad} . Note that T_{ad} depends on initial pressure P , initial unburnt temperature T_u , and composition of the reactants.

Variables:

$$H_P(T_{ad}, P) - H_R(T_u, P) = \sum_i n_i (h_{f,i}^0 + \int_{T_u}^{T_{ad}} \frac{c_{p,i}}{T} dT)$$

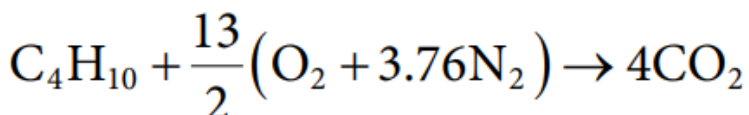
H_P is the total enthalpy of products at adiabatic temperature T_{ad} and pressure P . H_R is the total enthalpy of reactants at initial temperature T_u and ambient pressure. The Reactants; Chemistry components that react to a given state of heat transfers or combustion states. $h_{f,i}^0$ is the heat of formation of i th species, n_i is the number of moles of i th species ($C_{p,i}$) is the

specific heat of ith species that are dependent on temperature. the flame temperature of hydrocarbon–air is around 2200 + 100 K.

System at T_u (K)	P (MPa)	T_{ad} (K)
CH ₄ –air, 300 K	0.1	2200
CH ₄ –air, 300 K	2.0	2278
CH ₄ –air, 600 K	2.0	2500
CH ₄ –O ₂ , 300 K	0.1	3030
C ₄ H ₁₀ –air, 300 K	0.1	2246
H ₂ –air, 300 K	0.1	2400

the adiabatic flame temperature of the stoichiometric C₄H₁₀–air mixture at 298 K, 0.1 MPa, assuming no dissociation of the products for the following two cases: (1) evaluating CP of each species at 298 K, and (2) evaluating CP of each species at 2000 K.

$$C_4H_{10} + 13O_2 + 3.76 \times 13 N_2 \rightarrow 4CO_2 + 10H_2O + 45.2N_2$$



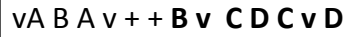
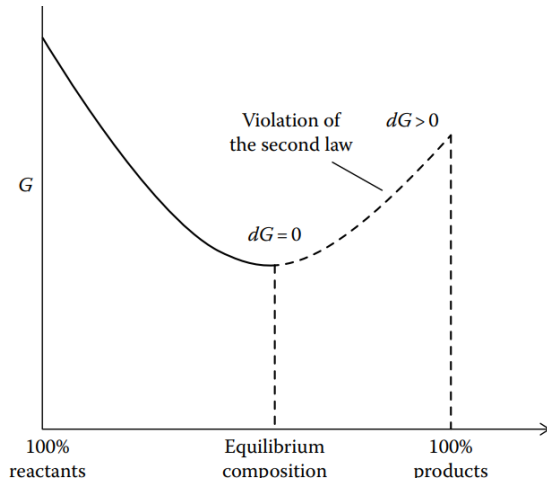
By differentiating the Gibbs function at constant pressure and temperature, we can have

$$dG = dH - TdS = dU + PdV - TdS = dU + PdV - TdS = 0$$

Let us now consider a homogeneous system involving chemical reactions for four chemical compounds, **A, B, C, and D**, at a given pressure and temperature. Let **n_A, n_B, n_C, and n_D**

the criterion of chemical equilibrium at a specified P and T.

Reactive process in **P & T**

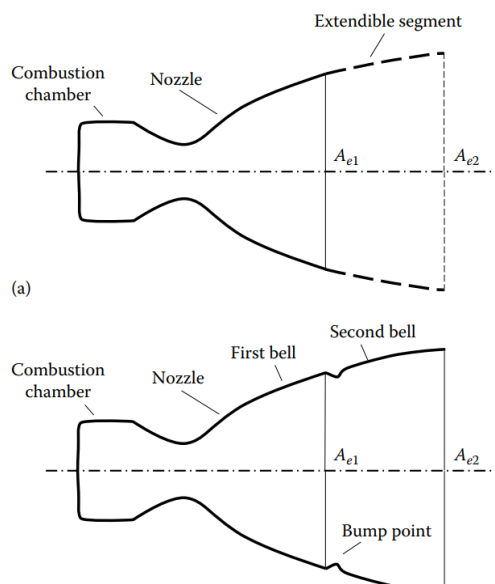


ν are stoichiometric coefficients. We can designate degree of reaction by $d\xi$ and change in the number of moles of any species during a chemical reaction can be expressed as:

$$dn_A = -\nu_A d\xi; \quad dn_B = -\nu_B d\xi; \quad dn_C = \nu_C d\xi; \quad dn_D = \nu_D d\xi;$$

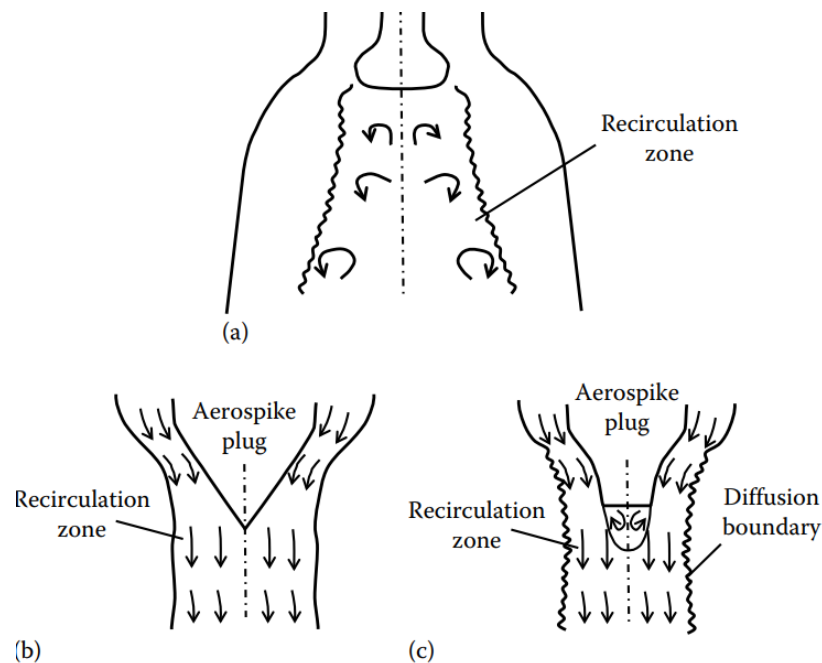
The minus sign indicates a decrease with the progress of the reaction. Similarly, the positive sign indicates an increase with the progress of the reaction.

Motor-reaction



(a) an extendible nozzle and **(b)** a dual bell-shaped nozzle. The extendible nozzle with a smaller exit area A_{e1} is used for a certain range of low altitude.

During low-altitude flight, the first bell nozzle segment with the smaller exit area A_{e1} is operated for the expansion of gas as the flow separation occurs at the hump point and does not adhere to the larger exit area A_{e2} . We need to calculate the variables of the relation area of the first bell, altitude, air and pressure. In contrast, at higher altitude, due to lower ambient pressure, gas expands further for a particular chamber pressure.



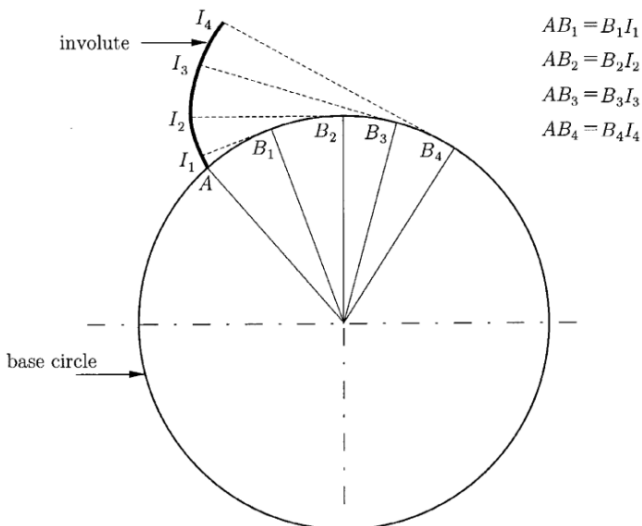
Schematic of (a) an expansion–deflection nozzle, (b) an aerospike nozzle, and (c) a truncated aerospike nozzle.

The expansion of gas flow around the aerospike gets adjusted directly with the changes in ambient pressure due to changes in altitude. At the designed pressure, the boundary will be almost parallel to the axis with similar performance as that of a conventional bell nozzle. But for higher ambient pressure, the boundary moves inward raising the exhaust pressure.

Thrust-vectoring(vectors)

The rocket nozzle produces thrust by expanding hot gasses only in a certain direction. But we need to change the direction of the thrust at the time of maneuver for which proper provisions have to be made in (a) Aerospike plug Diffusion boundary Recirculation zone (c) Aerospike plug Recirculation zone (b) Recirculation zone Schematic of (a) an expansion–deflection nozzle, (b) an

aerospike nozzle, and (c) a truncated aerospike nozzle. Propulsion the nozzle design. This is commonly known as thrust vectoring.

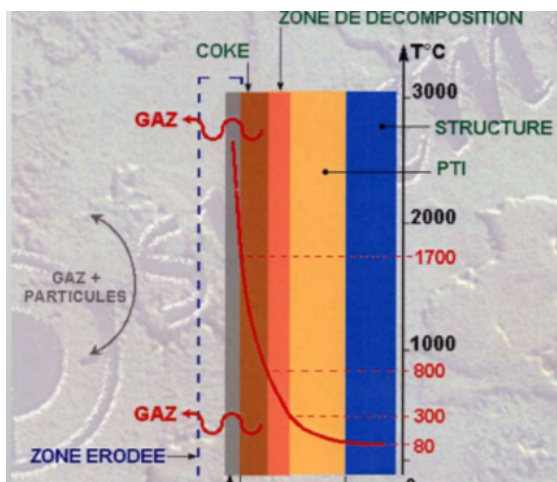


Chemistry-materials

Energy performance : I_{sp} , T_c , density

- Kinetic performances : maximum pressure, overall dimensions, weight
- Resistance to loads : shrinkage during curing, long-term storage, thermal cycles, firing
- Safety : resistance to mechanical or electrical aggression
- Resistance to aging
- Compliance with interface specifications
- Production cost

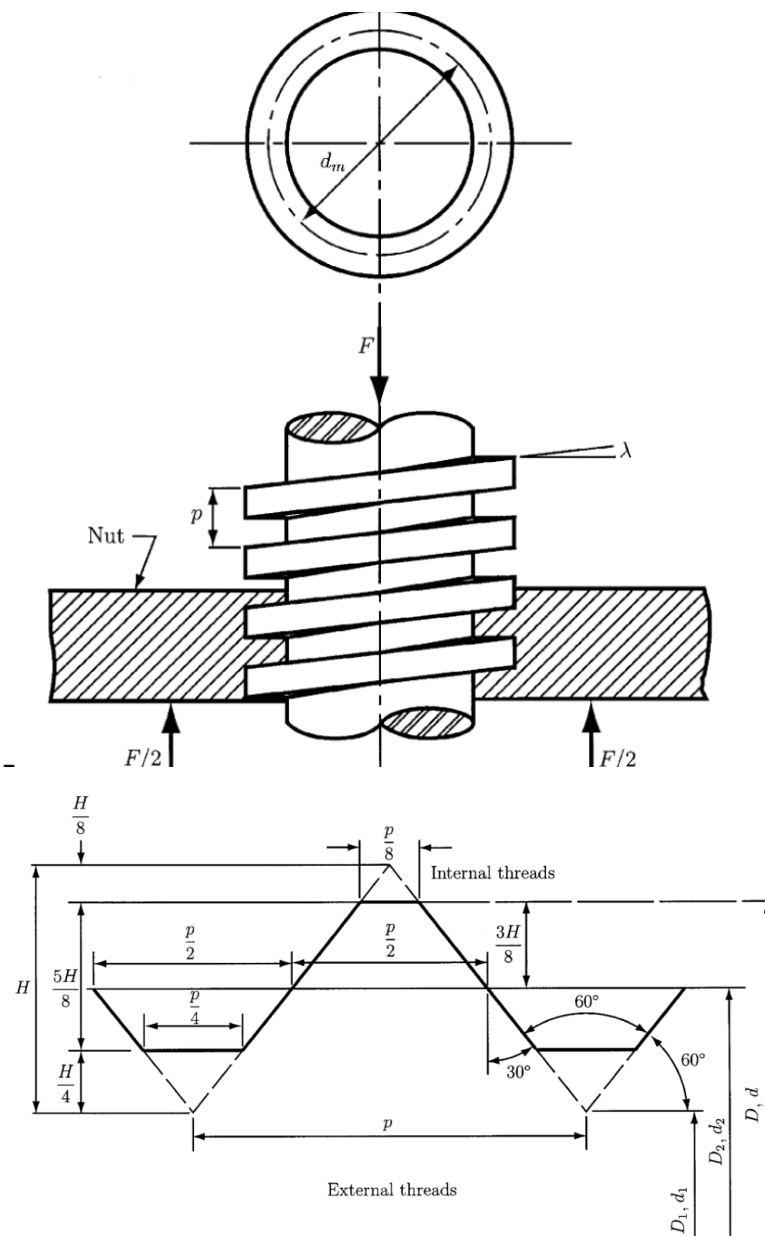
Diagram



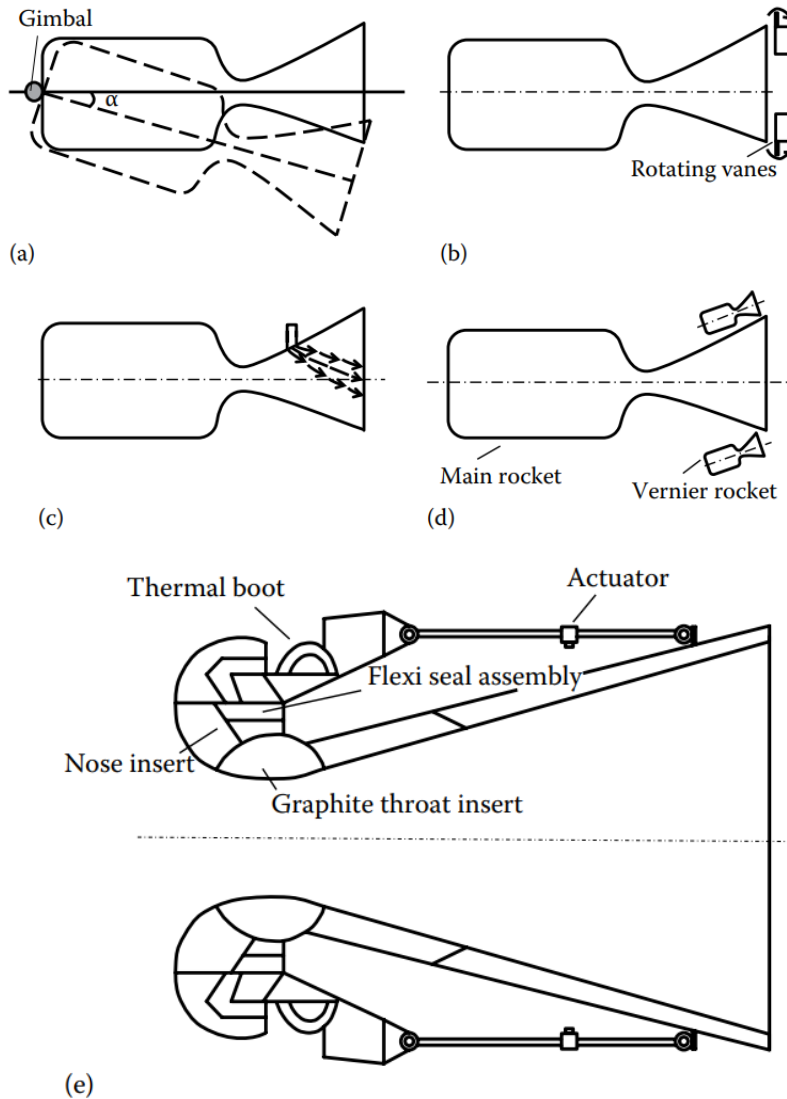
Mechanical-structures of rockets:

We need to evaluate the collision resistance materials, aluminum, titanium, steel, zone of inflexion of a given particular material after different launch-phases of the rocket. Chemistry Combined with the design of the metallic structures are cost effective for rocket design and propulsion logic. Also in this project, I want to include some additional steps integrating circuits for avionics, AVR sensors, Atmel microchips & programming into these chips.

Some examples of mechanical-metallic structures are:



In the gimbaling system, the entire engine is rotated using a universal joint. In summary; A hinge is permitted to rotate around each axis only using proper bearing such that thrust vectoring can be achieved. This calls for smaller control forces to execute the thrust vector, particularly for small changes in angle:



Side liquid injection: In this method, a secondary liquid is injected through the side wall into the main gas stream which forms an oblique shock in the diverging portion of the nozzle. The liquid jet must have sufficient jet momentum compared to the gas momentum in the diverging portion of the nozzle. This bow shock upstream of the cross jet causes the flow to separate from its wall due to a large pressure gradient. A recirculation is formed upstream due to this large pressure gradient. Strontium perchlorate with water solution (30:70) is preferred as a liquid

injectant. It is mostly preferred for small deflection. It is not favored for large side forces as large amounts of injectants have to be used.

Vernier rocket: Small auxiliary nozzles known as Vernier rockets are used to provide roll control of the rocket engine. These Vernier nozzles are small and can be actuated easily to deflect the exhaust nozzle flow.

Flexible nozzle: Among the recent types of nozzles, the flexible nozzle has found wider application for thrust vectoring, particularly for solid-propellant rocket engines as it does not reduce thrust and specific impulse significantly compared to other methods. A typical flexible nozzle submerged in solid propellant. The area ratio between the combustion chamber and the throat must be greater than 4 to have low velocity in the combustion chamber. But a smaller combustion chamber area is preferred due to constraints of rocket engine design. Nonuniform gas composition can cause losses due to incomplete mixing and combustion.

Pressure-performance:

-Performance of the rocket nozzle becomes slack during takeoff and burnout period due to transient pressure operation.

Variables:

1. Isentropic nozzle efficiency η_{in}
2. Discharge coefficient C_D
3. Thrust coefficient C_F

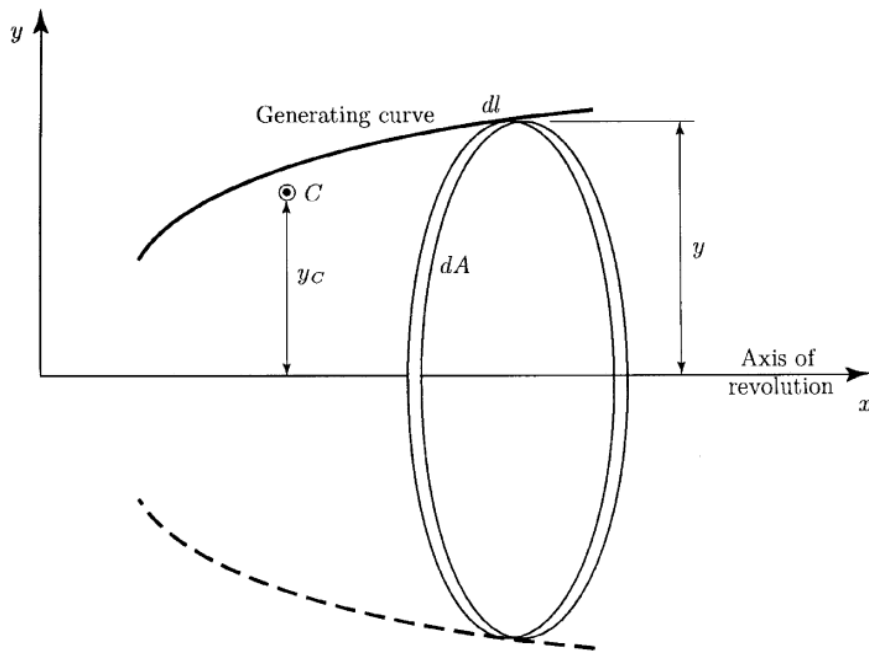
The velocity at the nozzle exit under isentropic expansion condition is higher than that in the non-isentropic condition due to increased entropy caused by friction, and turbulence effects. In order to ascertain the performance of the nozzle, efficiency is defined as the ratio of actual to isentropic enthalpy drop across the nozzle:

Variables to compute:

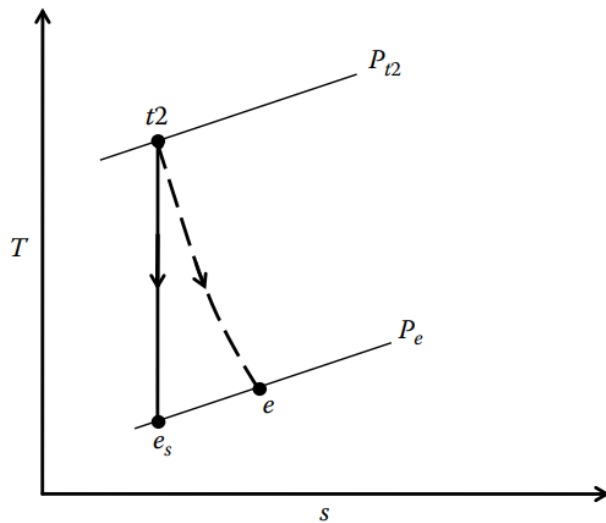
$\eta_{in} = \frac{h_{in} - h_{out}}{h_{in} - h_{out}^*}$

The isentropic efficiency can be evaluated knowing the pressure ratio, chamber temperature, and actual nozzle velocity. It takes care of various kinds of losses that make the flow non-isentropic. Its value lies from 90% to 95% depending on the flow condition, nozzle size and shape.

The expansion processes in a T-s diagram:



Several external forces, namely, thrust, aerodynamic forces (drag), gravitational forces, centrifugal forces, and coriolis forces, act on flying objects like a missile. The centrifugal and coriolis force being small in comparison to other forces



The thrust produced by the rocket motor usually acts in the opposite direction of the high-temperature, high-pressure gas that expands and exits from the rocket nozzle:

$$\mathbf{F} = m \mathbf{V}_p e$$

the propellant mass flow rate remains almost constant and thus can be expressed in terms of initial mass of propellant in the spacecraft and the burning time of the propellant t_b :

$$\dot{m} = \frac{m_p}{t_b}$$

The instantaneous mass of the vehicle m can be expressed as a function of the initial mass of the full vehicle m_0 and the propellant mass m_p at an instantaneous time t as follows:

$$m = m_0 - \dot{m} t$$

Gravity

Gravitational attraction acts on a space vehicle by all terrestrial bodies which pull the vehicle toward their center of mass. But when the vehicle is in the immediate vicinity of the earth, the gravitational attraction of other planets and bodies is negligibly small compared to the earth's gravitational force.

$$g = \frac{G M_e}{R_e^2} \left(1 - \frac{2h}{R_e} \right) \approx g_0 \left(1 - \frac{2h}{R_e} \right)$$

g_e is the acceleration on the earth's surface g is the local gravitational acceleration due to gravity **h is the altitude (km)** from the earth's surface R_e is the radius of the earth. rocket engine's flight, particularly within earth's atmosphere. The approximate expression for atmospheric **density ρ with altitude h** .

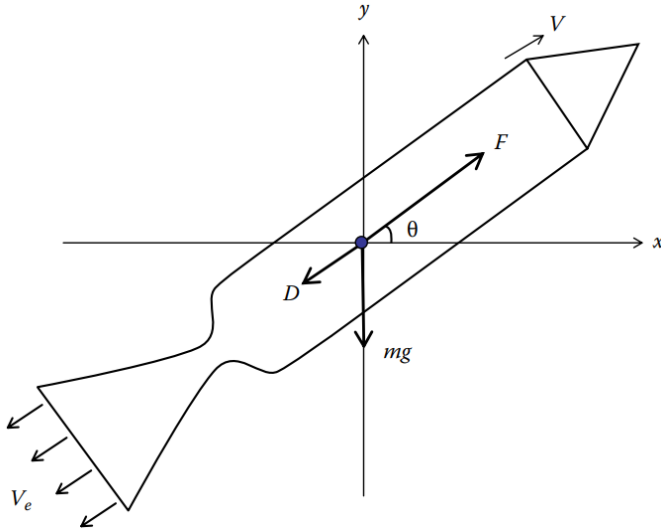
$$\rho = \rho_0 e^{-A h} \quad \text{relation with } A, B \text{ constants } (1.2 \text{ and } 2.9 \times 10^{-5})$$

A and B are constants whose values are 1.2 and 2.9×10^{-5} when density and altitude are expressed in SI units. During a flight the mass of the vehicle changes a great deal due to consumption of the propellant. When the rocket vehicle flies nearer the earth's surface, the gravitational pull of other distant heavenly bodies is small enough to be neglected. During this motion of the rocket vehicle, several forces, namely, thrust, gravitational force, drag, lift, control forces, and lateral force, and all moments will be acting on it, which might cause the vehicle to turn in a certain direction. As a result, the motion of the vehicle is inherently three-dimensional in nature.

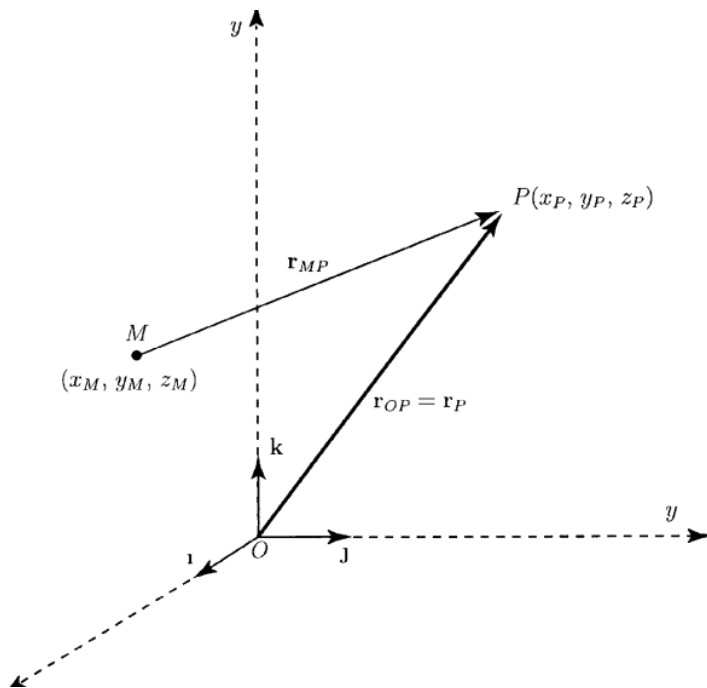
In the direction of the flight path, we know that the product of mass and acceleration is equal to the sum of all acting forces.

m is the instantaneous mass of the **vehicle** g is the acceleration due to **gravity** D is the drag force acting on the vehicle θ is the angle between the vehicle path and horizontal direction

A two-dimensional plane for a flying rocket engine vehicle.



t is the instantaneous time t_b is the total burning time m_p is the initial propellant mass m_0 is the initial mass of the vehicle **$PF = m_p/m_0$** is the propellant fraction:



The angle θ can vary continuously. The second term in the variables drag coefficients and densities that represents deceleration due to aerodynamic drag is difficult to integrate because we know that the drag coefficient C_D is a function of Reynolds number and Mach number. Besides this, C_D varies continuously with altitude, vehicle speed, and ambient density.

$$\frac{m(V) - m_b}{m_b} = \frac{1}{\cos \theta} \int_0^t \frac{g}{V} dt$$

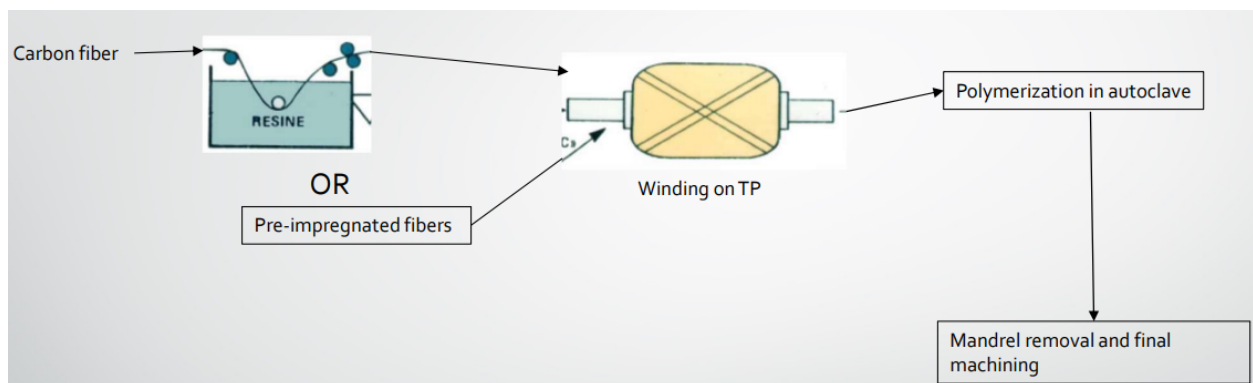
m_b is the burnout mass of the vehicle after all the propellant is consumed MR is the mass ratio of the vehicle. for certain missile applications, and the rest of the journey is in ballistic (free flight) mode.

$$\Delta V = V_{ex} \ln \left(\frac{m_0}{m_b} \right) - g t$$

m_b is the burnout mass of the vehicle after all the propellant is consumed MR is the mass ratio of the vehicle. The propellant gets consumed for a particular value of I_{sp} . Besides, it also depends on the exhaust velocity for a particular value of mass ratio MR, indicating how fast a propellant can be ejected from the exhaust nozzle. In order to have higher rocket velocity, the mass ratio MR must have a higher value.

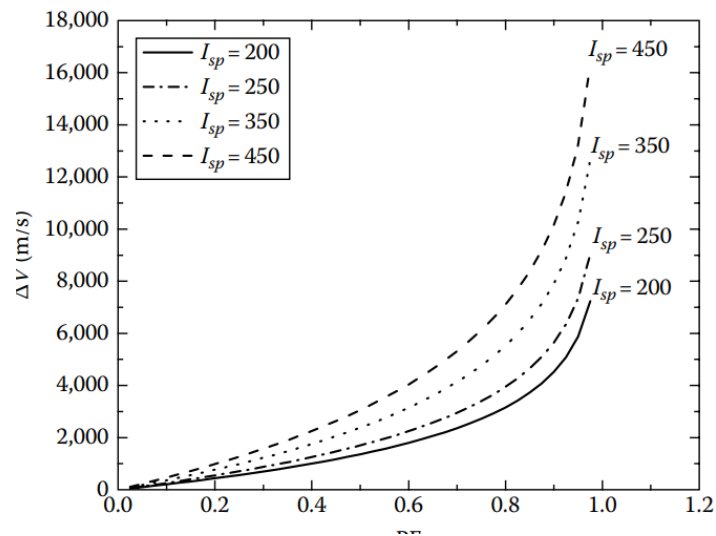
10% total mass of the vehicle is used for structure, empty propulsion system mass, payload, guidance, and control and control surfaces.

Materials for rockets



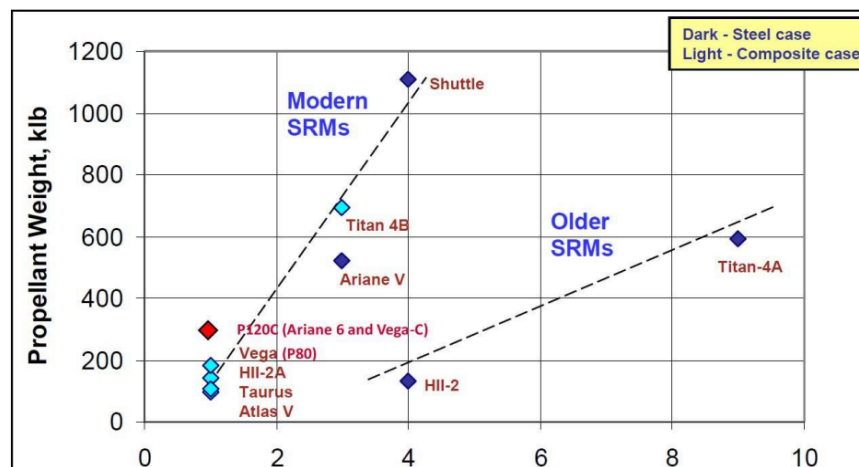
The design acumen of the rocket engine designer. In order to appreciate the dependence of I_{sp} and MR better, the variation in velocity increment is plotted for different and shrewd values of I_{sp} and exhaust velocity. It may be observed that the vehicle velocity increases asymptotically.

Variation of velocity increment with mass ratio MR:



When the rocket is fired vertically, we can neglect both the drag force and gravitational force acting on the rocket engine. We can determine the distance covered during the burnout period of the propellant, known as the burnout distance h_b .

Graphical use of propellant materials in rockets:



Gravitational-force description

The gravitational force F_g is balanced by the pseudo-centrifugal force $m\omega^2 R$. The angular velocity ω and orbital velocity V_o . The orbital velocity decreases nonlinearly with the radius of the orbit. The time period per revolution increases with the radius of the orbit at a higher rate

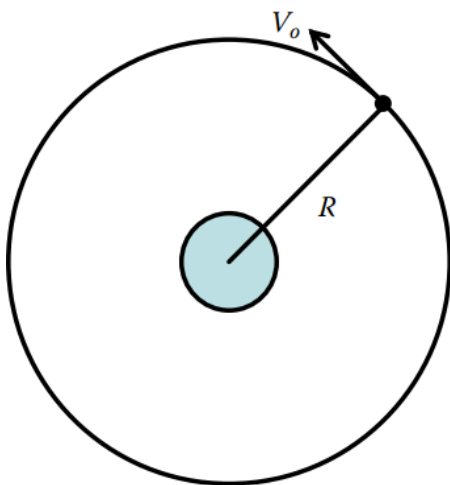
compared to the orbital velocity. An example could be: a satellite that is placed at a height of 250 km from the surface of the earth in a circular orbit.

Law of ellipse: The path of the satellite about the planet is elliptical in shape, with the center of the planet being located at one focus.

2. Law of equal area: The imaginary line joining the center of the planet and the center of the satellite sweeps out an equal area of space in equal amounts of time.

3. Law of harmonies: The ratio of the squares of the periods of any two satellites is equal to the ratio of the cubes of their average distances from the planet.

Orbital velocity with radius R :



Motor Flow Instabilities:

It is useful to consider the equation for a simple oscillator of state variable p , where dot indicates time derivative, α the linear damping coefficient, ω the angular frequency and $F(t)$ a forcing function:

$$\ddot{p} + 2\alpha \dot{p} + \omega^2 p = F(t)$$

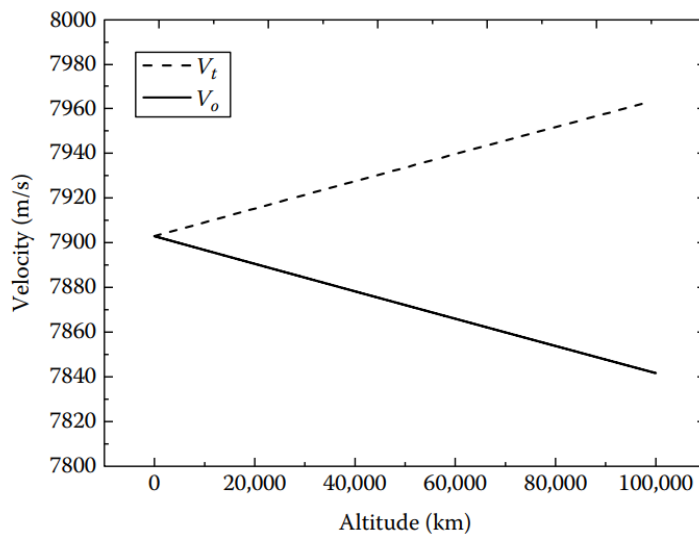
$$F(t) = F_0 \cos(\omega t + \phi)$$

To calculate motor Instabilities at the time that the rocket is expend the fuel and other material consumption:

orbits need not to be circular always; rather they can be elliptic. When a spacecraft is orbiting in a circular orbit, if its velocity decreases, it can enter into an elliptic orbit. It may be noted that a planet is located at the focal point of the ellipse while the satellite is orbiting at an orbital velocity of V_o . In a polar coordinate system, an elliptical orbit is described by the instantaneous radius R from the center of the planet, and the major axis a and minor axis b .

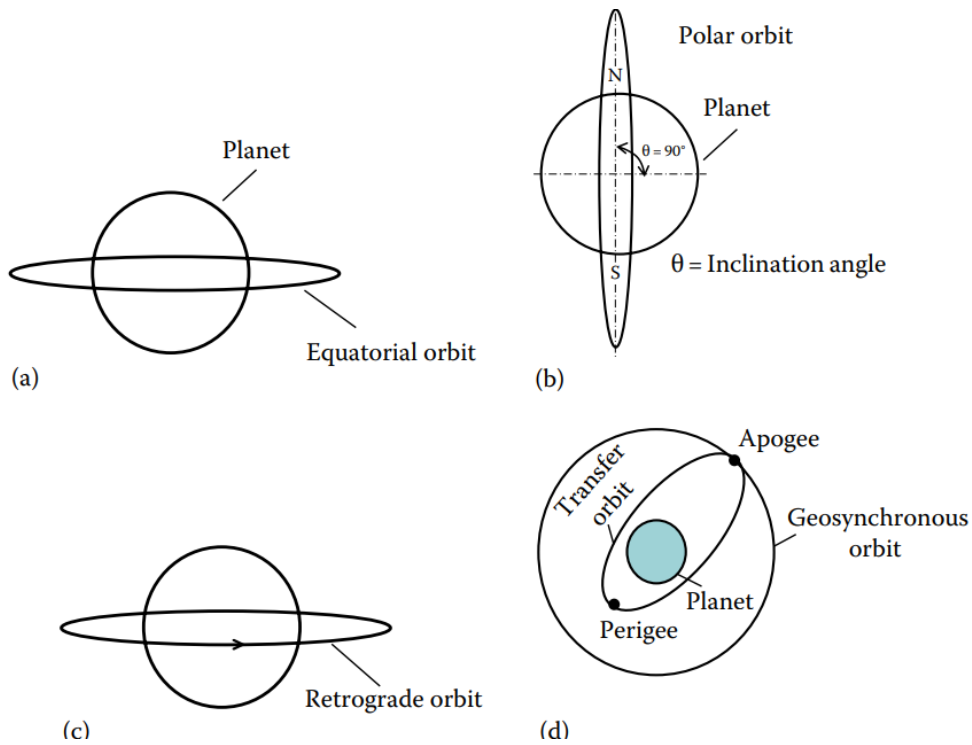
The acoustic balance method was first proposed by Hart & McClure [3] and was given its most practical form by Culick [4-6]. The acoustic balance technique belongs to the asymptotic expansion methods. Every variable F is split into its mean, \bar{F} , and fluctuating, F' , parts:

$$F = \bar{F} + F' \text{ with } \epsilon = F' / \bar{F} \ll 1.$$



ϵ	\bar{M}	Problem
0	\bar{M}	Steady, incompressible flow
ϵ	0	Acoustic, without mean flow
ϵ	\bar{M}	Linear coupling: mean flow-acoustic

ϵ is a perturbation parameter that characterizes the instability and is used to split the governing equations into successive powers of ϵ . A second perturbation parameter, \bar{M} , representing the mean flow Mach number, is used to simplify the equations. Assuming $\bar{M} \ll 1$ implies that the mean flow remains incompressible, which is a good approximation in the combustion chamber



Unstable amplitudes for rocket parametrization

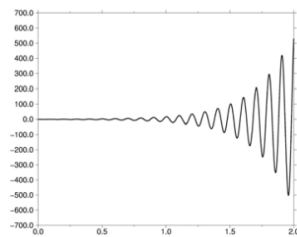


Figure 2-a: Linearly Unstable.

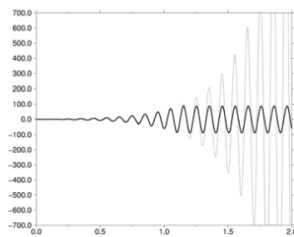


Figure 2-b: Harmonically Forced Linearly Unstable and Non-Linearly Stable ($\alpha > 0$ for Large Amplitudes).

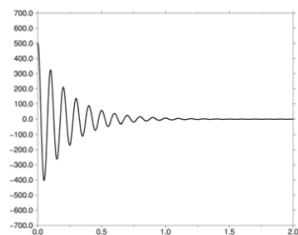


Figure 2-c: Linearly Stable.

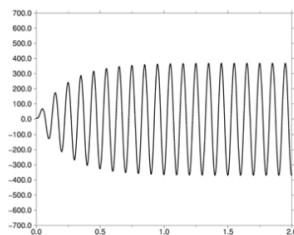
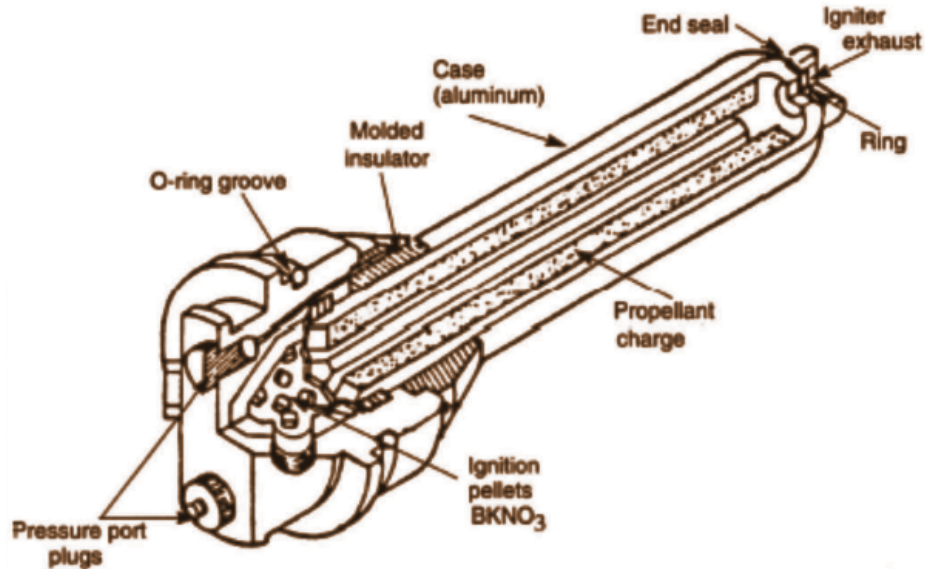


Figure 2-d: Linearly Stable, Harmonically Forced.

Instability in rocket amplitudes varies in the order ϵ . M is the lower order that permits the description of the instabilities and corresponds to linear equations in ϵ . As a consequence, only

the tendencies of infinitesimal perturbations to grow or decay can be determined in the form of a damping coefficient α ($F' \propto e^{-\alpha t}$)



Since most motors use metallized propellants, the combustion products carry some amount of condensed phase products, such as alumina droplets. These will add to the motor stability. In fact, one of the reasons to load propellants with metal powder, such as aluminum, is to increase the stability of the motors (another reason being the benefit of increased specific impulse).

From what precedes, it is clear that some sources of instability are missing from the acoustic balance approach. Flandro and Jacobs were the first to mention the “vortex-shedding” as a possible additional driving to the motor stability balance.

Magnitudes & correlations with variables in acoustic instabilities:

Present interesting attempts to use correlations of this type. However, it must be stressed that such correlations have a limited predictive merit and can be compared to the celebrated “age of the captain” formula (mast height divided by the ship speed): all the difficulty lies in the proportionality constant which has no universal quality. Reference [20] goes one step further in using the Rossiter’s formula to correlate the observed frequencies. This approach uses the relative time delays of the vortex emission to the acoustic feedback. The figure hereafter illustrates this point of view.

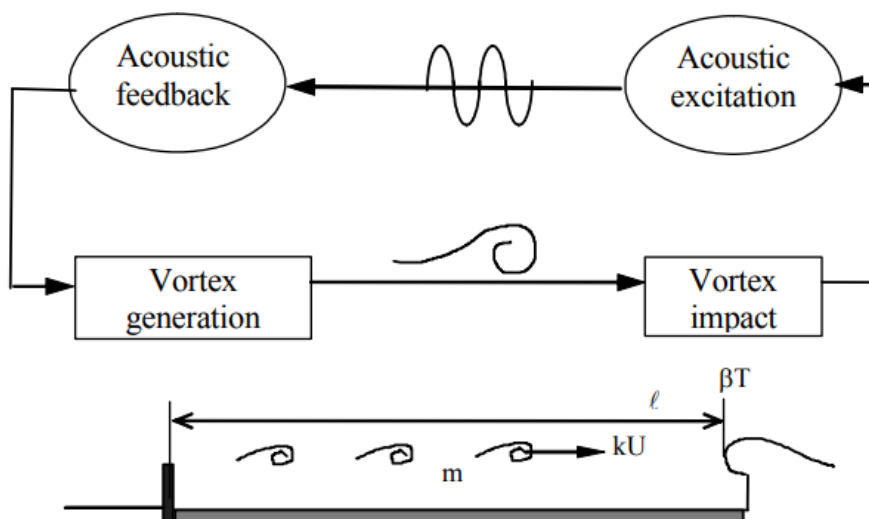
Let T be the time period of the vortex-shedding, k the ratio of vortex displacement velocity to the mean axial flow velocity, U , β an empirical constant representing the time delay between vortex impact and acoustic wave emission and m the number of vortices on distance l .

Observable vortices are the results of a non-linear growth process. As a consequence, our knowledge of such vortices and of their dependencies on the known parameters is blurred by the non-linear growth stage of initial unstable vortical waves, a process which most of the time remains beyond our present understanding. However it is of major importance to better understand the initial destabilization mechanisms, simply because they have definite frequency signatures and sensitivities to flow characteristics which must be known in order to understand their potential effectiveness to couple with acoustic waves and produce harmful vortices.

$$mT = l/kU + l/c + \beta T$$

Model

The combustion of aluminum droplets carried by the flow, the structure motions (as possibly affecting the mean and unsteady flows). Finally, the model should be able: a) to propagate the acoustic waves, b) to describe the details of the internal flow, including the capture of acoustically forced vorticity waves as well as flow instabilities and their non-linear growth, c) to include some form of condensed phase model (inert and reactive), d) to couple with propellant combustion models, e) to couple with solid mechanic models.



Analysis for motors in rockets

Analytical solutions of unstable flow regimes, Dedicated lab scale motors with high quality and numerous measurements to gain real firing tests data, Meticulous characterization efforts to provide the model inputs. These comprised condensed phase characterizations, details of the propellant composition, including characterizations of AP and aluminum size distributions, and unsteady propellant combustion responses function determinations, Dedicated models for combustion mechanisms and fluid-structure couplings, Dedicated and documented test cases for model evaluations.

Vortices-oscillations-waves

The vortical origin of these oscillations can be traced to their particular frequency signatures. Indeed it was observed that instabilities followed peculiar frequency tracks, showing decreasing frequencies and sudden jumps around the pure acoustic frequency. For example, the figure below shows the time evolution of the head end pressure power spectral density for one subscale firing. The particular frequency tracks around chamber acoustic mode frequencies (solid lines)

Variables to measure constants and speeds across instabilities and the frequencies in a rocket propulsion stages:

- P, T and ρ : respectively pressure, temperature and density
- V : gas flow velocity
- A : cross section of the nozzle
- R : universal gas constant $r = \frac{R}{\mathcal{M}}$
- a : the speed of sound $a = \sqrt{\gamma r T}$
- M : the Mach number $M = \frac{V}{a}$

And the following equations :

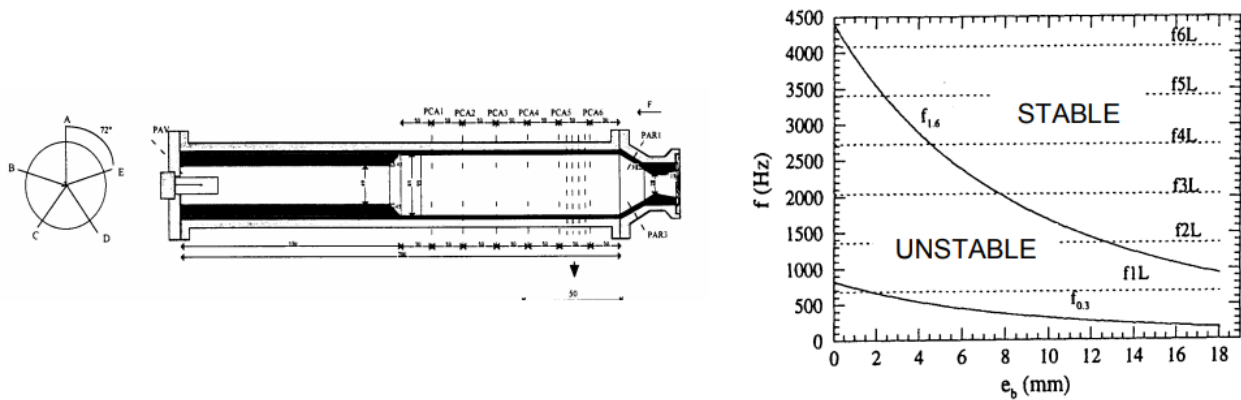
- The Mariotte law : $\frac{p}{\rho} = r \cdot T = \frac{R \cdot T}{\mathcal{M}}$
- The continuity equation : $\rho \cdot V \cdot A = \text{constant}$
- The energy conservation equation : $V^2 = 2 \cdot c_p \cdot \Delta T$.
- The Mayer formula : $c_p - c_v = r = \frac{R}{\mathcal{M}}$

The decrease of the frequency during motor burn was viewed as an indication of the driving being the result of flow instabilities, linked to the mean flow axial velocity. Indeed in most solid propellant motors the axial velocity continuously decreases, due to increasing motor port area, as propellant burns out.

Decreasing frequency tracks with sudden jumps are clearly visible and indicate that the observed instabilities belong to flow driven instability regimes.

In order to devise a whistling motor, one has to verify that:

- a) the most unstable frequency of the vortical waves matches the chamber longitudinal acoustic mode frequency,
- b) the stand-off distance separating the vortex emission point to the interaction point, assumed to be localized at the nozzle entrance, is sufficient to contain an integer number of vortices of wavelength λ_v . These two conditions are necessary conditions to produce vortex driven instabilities.



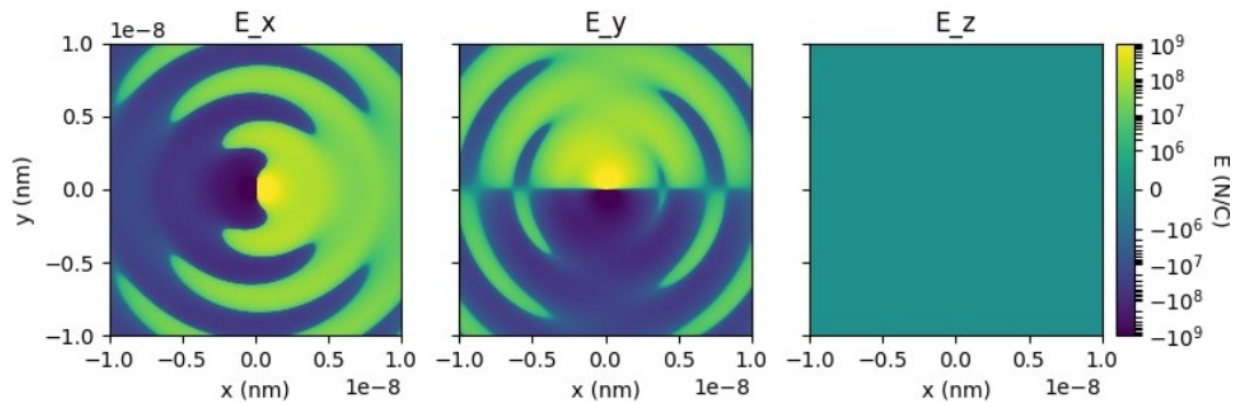
The acoustic frequencies never match the most amplified frequency, it was anticipated that the motor would be unstable. Indeed, a coupling path is available since the acoustic frequency of the first mode lies in the range of the shear layer unstable frequencies. In that vision, the shear layer is a mere broadband amplifier and will naturally tune to available frequencies.

the acoustic balance approach described earlier, amplitudes were not always decreased by the presence of condensed phase) it was limited by the difficulties in characterizing the propellant combustion response.

function $p'(\cdot)$ $p m'(\cdot)$ $m R M P(\cdot)$ $\omega \omega \omega = \& \& .$

As an example, the following parameters have been fixed : $R = 1000$, $x = 10$ and $\alpha = 4$. Some eigenvalues are plotted in figure 3.1 in the complex ω -plane. The horizontal line $\omega_i = 0$ separates the instability zone from the stability zone. The higher the points are, the most

dangerous they are (according to the temporal theory). In the instability region, only two amplified modes have been found : $\omega \in \{31.59 + 1.6946i, 31.622 + 1.6296i\}$

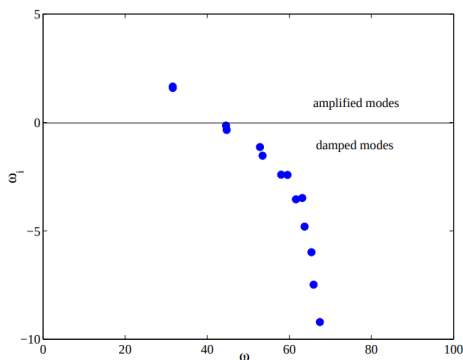


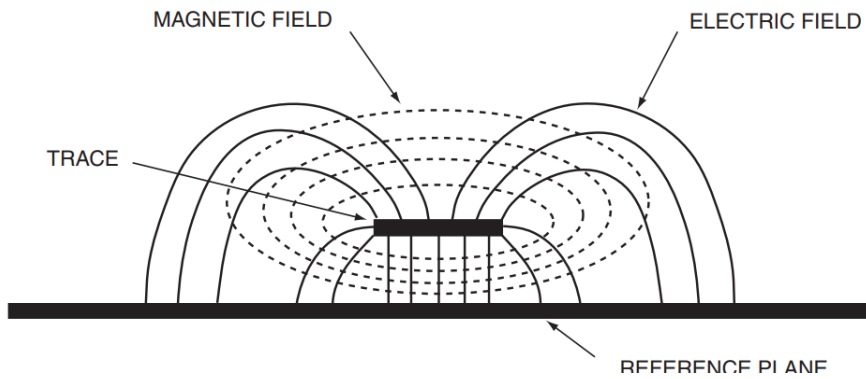
Circuit implementation analysis

After considering waves, acoustic instabilities & other factors in rocket design we can consider That in this section, we can represent the implementation of circuits and algorithms for rockets To continue one special union between the hardware parts design, the software behind the circuits and the algorithms to make the rocket alive in other forms. The final objective of this text is to make rocket launch stages more easier to test and circuitry implementations taking in consideration acoustic problems and mechanical designs.

Magnetic-Vectors

We need to elaborate effective and functional algorithms to develop stronger and fast reliable products based on circuits and mechanical systems in the magnetic and electronic field and implement these fields into the mechanical systems to develop less cost consumption energy electronic and robotic products.



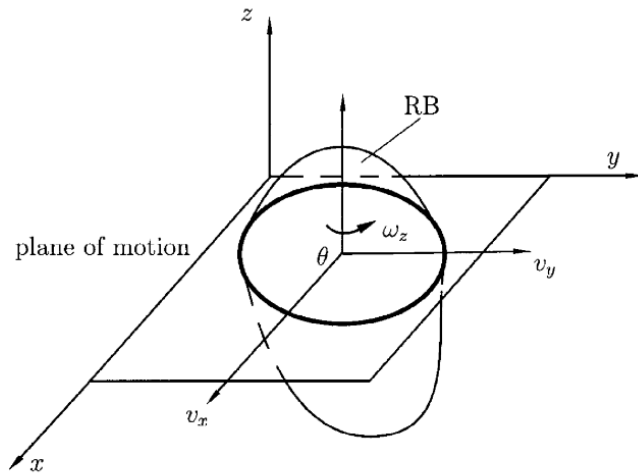


```

cycle 1: start  $x_A \cdot z_B$ ; start  $x_B \cdot z_A$ ;  $z_B := x_A + z_A$ ;
cycle 2:  $z_B := z_B^2$ ;
cycle 3:  $z_B := z_B^2$ ;
wait until (done1 and done2) = 1;
cycle i:  $R := x_A \cdot z_B$ ;  $x_B := x_B \cdot z_A$ ;
cycle i+1: start  $x_A \cdot z_A$ ; start  $R \cdot x_B$ ;  $z_A := R + x_B$ ;
wait until (done1 and done2) = 1;
cycle j:  $x_A := x_A \cdot z_A$ ;  $x_B := R \cdot x_B$ ;  $z_A := z_A^2$ ;
cycle j+1: start  $x_P \cdot z_A$ ;  $R := x_A^2$ ;
wait until done1 = 1;
cycle k:  $x_A := x_P \cdot z_A$ ;
cycle k+1 :  $x_A := z_B$ ;  $z_A := R$ ;  $x_B := x_A + x_B$ ;  $z_B := z_A$ ;

```

Z_1 is one vector acting on the circuits surface
 Z_1 and Z_2
 $V_1 + V_2 = V'$
 $Z_1 * I + Z_2 * I = Z(eq) * I$
 $Z(eq) = Z_1 + Z_2$
 $Z(eq) = \text{SUM}(n) \text{ components}(i=1) \text{ integrating vector } Z_1$
For each variable $Z(i)=R + j X_i$



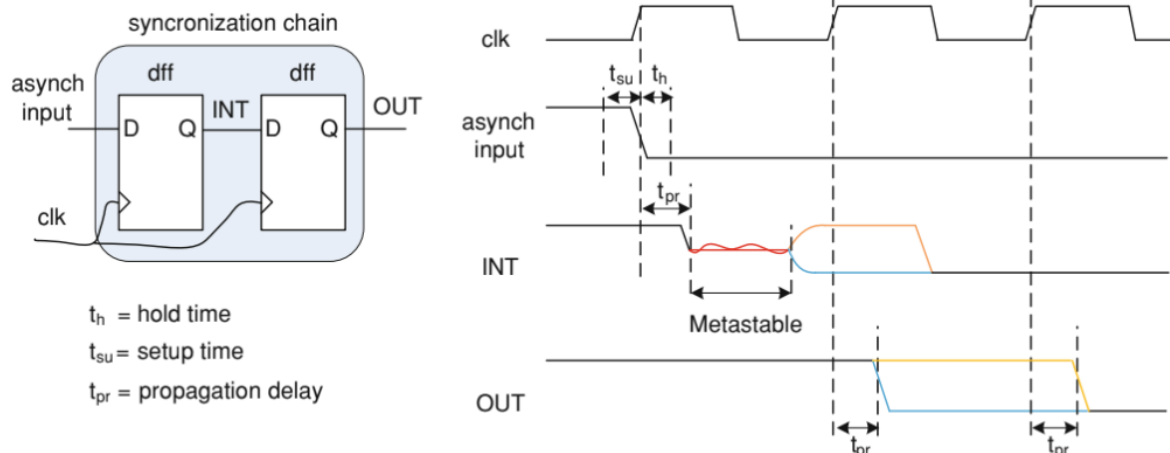
For each variable $Z(i) = R + j X_i$

$Z(eq)$ we have to sum the real parts $R(i)$ and the imaginary $X(i)$ on the other side. The terms $X(i)$ can be reactions of the other variable form $wL(i)$ in the circuit system $-S+_{-}$

$I(i) = V/Z(i)$
 the Generator for waves is
 $I = \text{SUM}(n \text{ components and } i=1) = \text{Vector}/Z_i + \dots + \text{Vector}/Z(n)$

Parallel connections support these kinds of math systems:

$Y(\text{vector}) = G + jB$
 $I = (Y_1 + Y_2 + \dots + Y_n)V$
 $I = Y(eq) * \text{Vector}$
WAVES:
 $Q = Xl(\text{square})$
 $p = I(\text{square})R$ or $P = V(R)I$



The active power P produces an effective work in the ohm resistances, motors for rockets in the case of a simulation example with Pyrocket in python to model motors.

P power for motors are measured in (W)

The circuit C is equivalent to these variables:

IT, I1,I2,I3,P,Q,S, FP for any vectorial diagram with OHMS

and waves systems for circuit design. The intensity of the forces that interact with circuits are charges in one (S) system across the conductors in time units described in $v * t$

Segment 1. If N is the number of particles, $Q=Nq=nV * q$,

V is the volume specification in the conductor system for waves and circuits C.

Signal processor to organize and calculate frequencies;

The single board computer is feeding a pre-recorded RF dataset to a DAC channel on the VP431.

This DAC channel creates an RF signal which is looped back via an RF cable to an ADC channel on the VP431.

The ADC samples the incoming RF signal and performs a digital down conversion step before placing the sample data into a memory buffer in the FPGA. This data is then moved to Intel CPU memory on the SBC3511 via the PCIe interface using a DMA transfer. The data then goes through a signal processing stage on the Intel CPU to compute the power spectrum of the RF signal. This power spectrum is then displayed in a rolling 3D waterfall plot, utilizing the Intel GPU and Abaco AXIS tool suite.

The diagram illustrates the SCS 1000 architecture, showing the connection between various VPX modules and the system backplane.

VPX Modules:

- VPX 1: RF PAY SPARE
- VPX 2: RF PAY SPARE
- VPX 3: TIM SLOT SPARE
- VPX 4: DATA & CONTROL PLANE SWITCH (SWH SWE440S) with Switch MNGT interface
- VPX 5: SEC PAY SPARE (CP, DP)
- VPX 6: RF PAY VP431 (CP, DP, EP)
- VPX 7: RF PAY SPARE (CP, DP)
- VPX 8: I/O PAY SBC3511 (CP, EP, IO)

Other Components:

- POWER SUPPLY 1400W
- SSD
- Aperture H (multiple)
- Aperture
- VITA 67.3c
- Meritec FP

Connections:

- VPX modules are connected to the SCS 1000 Backplane - Elma 1SVX308ABP-1X31.
- The backplane connects to the Aperture H and Aperture modules.
- The Aperture module connects to the VITA 67.3c module.
- The VITA 67.3c module connects to the Meritec FP module.
- The Meritec FP module connects to the I/O PAY SBC3511 module.

Legend:

- EP: x4 Gen 3 PCIe (FP)
- General purpose IO
- CP 1000BASE KX, 10GBASE KR ethernet (UTP)
- DR: 40GBASE KR4 (FP)
- IO: SFP+ 10/1GbE
- ADC IN
- DAC OUT

SBC IO via Meritec: Serial, USB, DisplayPort, 1000BASE-T

SOSA Slot Profiles:

- RF PAY: SLT3-PAY-1F1U1S1U1U2F1H-14.6.11-9.2
- I/O PAY: SLT3-PAY-1F1U2U1U1U1U1U1U14.2.16
- SEC PAY: SLT3-PAY-1F1U1S1U1U2F1H-14.6.11-9.2
- TIM: SLT3-TIM-2S1U2S1U2U1U1H-14.9.2

The diagram illustrates the P1000 system architecture, which is a 1U rack-mountable server. The main components and their connections are as follows:

- System Board (P1000):** The central component, featuring a **CPU Xeon E** (32 GB DDR4 with ECC), **PCH (CM246)**, **FPGA (Ultrascale+)**, and **RAM** (32 GB DDR4 with ECC).
- Storage:** Includes **NVMe SSD** (x4 Gen3), **SPI Flash** (BOOT, RECOVERY, FSP), **NVRAM** (1 MB (BIT/User), 1 MB (HM)), and **TPM 2.0**.
- Networking:** Features a **Dual NIC** (1G/10G/40G Ethernet) and **10G-KR Ethernet** ports.
- Expansion:** Includes **PHY** and **MAG** components for expansion.
- Connectivity:** Supports **IPMI x2**, **x4 PCIe Gen3**, **40G-KR4**, **10G-KR**, **XMC (12d)**, **COM1**, **1000BASE-T**, **USB3 x1**, **USB2 x1**, **SATA x1**, **XMC (8d + 16s)**, **COM2 / COM3**, and **DisplayPort**.
- Other Components:** Includes **SPI Flash (BOOT)**, **SPI Flash (RECOVERY)**, **SPI Flash (FSP)**, **NVRAM**, **TPM 2.0**, **IPMC**, **IMPB x2**, **COM 1**, **10G-KR Ethernet**, and **HM Sensors**.

- Xeon E CPU (E-2276ME) formerly known as Coffee Lake Refresh
- **6-cores at 2.8 GHz**
- 45W TDP
- **CM246 PCH (Platform Controller Hub)**

SDRAM

- **64 GB DDR4 SDRAM (dual channel)**

soldered with ECC
Non-Volatile RAM

- **1 MB FRAM (BIT / User)**

On-board NVMe Solid State Disk Drive (SSD)

- Up to 256 GB

BIOS

- **2x 32 MB SPI Flash for BIT and BIOS**

plus 1x 32 MB SPI Flash for Recovery Data Plane

- 40GBASE-KR4

Expansion Plane

- **Four lanes of Gen 3 capable PCIe to P1**

Control Plane (Gigabit Ethernet)

- **ETH0 is always present, configured as 1000BASE-T (VPRO-compliant), and routed to P2**
- **ETH1 and ETH2 are routed to P1 and configured as 10GBASE-KR by default.**

Another specifications for radio frequency;

Watchdog/ Timers/ TPM/ ETI

- **Software programmable windowed**

watchdog in FPGA

- Timers in FPGA (software programmable)

- **TPM 2.0 (Trusted Platform Module)**
- ETI (Elapsed Time Indicator)

Temperature Sensor

- **PCB and FPGA temperature sensors**

FPGA

- Xilinx Zynq UltraScale+ FPGA (ZU5EG) with advanced security features

Atmel microcontroller for aerospace systems

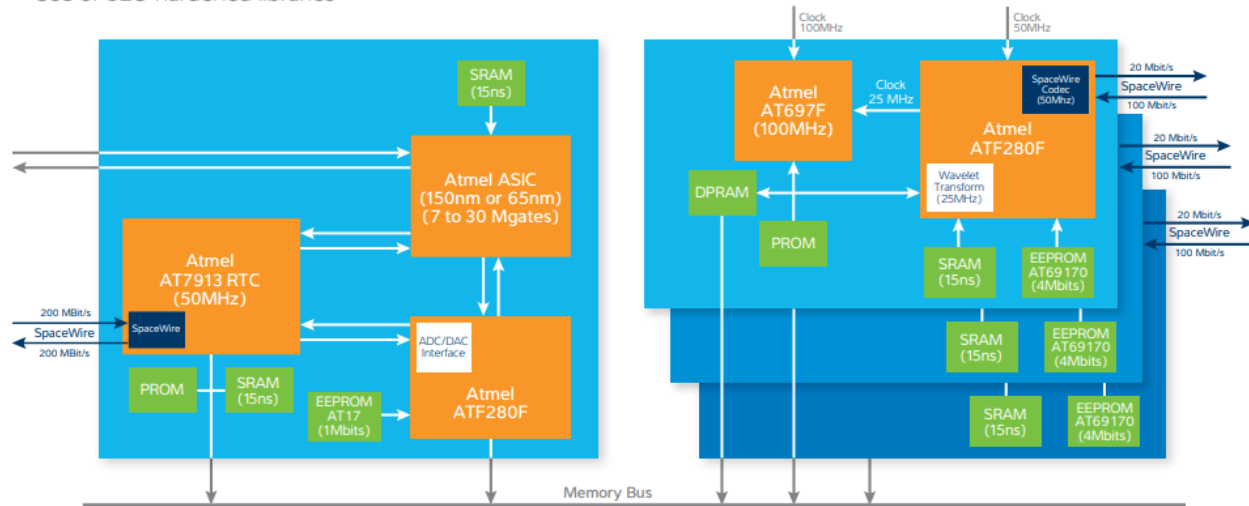
- The Atmel aerospace design flow uses a validated sequence of tools from RTL to GDSII.
- Cadence Floor planning, layout prototyping, signal integrity, package design Synopsys Logic/physical/test synthesis,
- physical design, power analysis,
- static timing analysis,
- formal verification,
- cell characterization tool Mentor Graphics Logic simulation, test synthesis,
- DRC/ARC/LVS verification Magma Library cell characterization Atrenta

- Power optimization, DFT, SDC/CDC verification at RTL level Ansys Power integrity

Connecting Space Systems

Atmel SpaceWire value for space applications

- Compliant with the SpaceWire standard ECSS-E-ST-50-12C
- Flight Heritage in ESA, NASA, JAXA missions
- Use of SEU hardened libraries
- QMLQ & QMLV space grades with SMD
- Insure System interoperability



Space-Memory locations

Part Number	Type	Process Feature Size (μm)	Format	Operating Voltage (V)	Prime Speed Spec (ns/mA)	TID (Krad)	Package
AT65609EHV	SRAM	0.35	128K x 8	4.5 – 5.5	40/50	300	FP32.4 SB32.4
M65609E	SRAM	0.35	128K x 8	3.0 – 3.6	40/50	300	FP32.4
AT60142HT*	SRAM	0.25	512K x 8	3.0 – 3.6*	17/170	300	FP36.5
AT60142H	SRAM	0.25	512K x 8	3.0 – 3.6	15/170	300	FP36.5
AT68166HT*	MCP SRAM	0.25	512K x 32	3.0 – 3.6*	20/170	300	CQFP68
AT68166H	MCP SRAM	0.25	512K x 32	3.0 – 3.6	18/180	300	CQFP68
M67025E	DPRAM	0.6	8K x 16	4.5 – 5.5	30/200	30	CQFP84
M67204H	FIFO	0.6	4K x 9	4.5 – 5.5	15/120	30	FP28.4
M67206H	FIFO	0.6	16K x 9	4.5 – 5.5	15/120	30	FP28.4
M672061H	FIFO with programmable HFF	0.6	16K x 9	4.5 – 5.5	15/120	30	FP28.4
AT28C010-12DK	Parallel EEPROM	0.6	128K x 8	4.5 – 5.5	120/80	30	FP32.4
AT17LV010-10DP	Serial EEPROM	0.35	1M x 1	3.0 – 3.6	100/10	60	FP28.4
AT69170E	Serial EEPROM	0.18	4M x 1	3.0 – 3.6	70/15	60	FP18.3